

ECODYNAMIC ASSESSMENT OF THE SUBMERGED AQUATIC VEGETATION IN LAKE OKEECHOBEE, FLORIDA UNDER NATURAL AND ANTHROPOGENIC STRESS

NI-BIN CHANG¹ & KANG-REN JIN²

¹Department of Civil, Environmental, and Construction Engineering, University of Central Florida, Orlando FL, USA.

²South Florida Water Management District, West Palm Beach, FL, USA.

ABSTRACT

Lake Okeechobee, a large, shallow lake in southern Florida, is the liquid heart of the Everglades. The lake's hydrodynamic patterns and water depths have been impacted by four major hurricanes in the past decade, including Irene (1999), Frances and Jeanne (2004), and Wilma (2005), and intermittent water level variations due to droughts in 2000–2001 and 2007–2008. In the past few decades, conditions in Lake Okeechobee have changed significantly, largely as a result of nutrient inputs to the ecosystem from agriculture and other human activities in the watershed. The excessive phosphorus loads from the lake's watershed have led to an increase in eutrophication and contributed to the accumulation of phosphorus-rich mud sediments on the lake bottom. The cumulative effect of these continuous natural hazards and anthropogenic impacts in Lake Okeechobee resulted in resuspending a large quantity of sediment, lowering light transparency, and releasing a large amount of nutrients into the water column, followed by long-standing shallow water depths. Such collective impacts led to a drastic change of sediment bed and ecosystem stability, especially the submerged aquatic vegetation (SAV). This study quantifies the ecodynamics of SAV to elucidate the coupled impact of natural and anthropogenic stress by a numerical model, the Lake Okeechobee Environment Model (LOEM) that links the spatial and temporal distributions of SAV as a whole.

Keywords: anthropogenic impacts, ecosystem dynamics, lake sustainability, natural hazards, sediment bed, water quality.

1 INTRODUCTION

Lake Okeechobee, the second largest freshwater lake (1,730 km²) in the continental United States, is located around 27° N latitude and 81° W longitude. The lake was formed about 6,000 years ago and is very shallow with an average mean depth of about 2.7 m. Surface elevation has varied from 2.6 m (8.82 feet, NGVD29) to 5.7 m (18.77 feet, NGVD29) over the past seven decades [1,2]. Surface inflow, outflow, and lake level are managed for the competing needs of water supply in urban areas, ecosystem conservation of coastal estuaries, regional flood control, flood protection, and irrigation for agricultural land. The lake itself is a critical habitat nature area for fish, birds, and other wildlife in the United States [3]. Lake Okeechobee, bounded by the Herbert Hoover Dike, is turbid and eutrophic, largely due to nutrient inputs to the ecosystem from agriculture and other human activities in the watershed during the past few decades. The excessive phosphorus (P) loads from the lake's watershed have led to an increase in eutrophication and contributed to the accumulation of P-rich mud sediments on the lake bottom [4]. P-laden sediment is regularly resuspended back to the water column due to wind and wave actions. Resuspended mud sediments can be a primary source of P to the water column, which may outweigh external load reduction efforts [5,6]. The contribution of P to the lake's water from internal loading may be affected by changing pH values in the lake. The major cause of sediment resuspension in Lake Okeechobee is associated with the bottom shear stress resulting from wind-generated surface waves [7]. This implies that surface waves generated by local wind gusts and hurricanes may quickly propagate to the lake's bottom and generate bottom shear stress to suspend the sediment particles.

Table 1: Hurricane winds and bottom shear stress in Lake Okeechobee [8].

Hurricane name	Landfall location (Florida)	Peak date	Sustained wind speed (m s^{-1})	Persistent time (days) ($\geq 8 \text{m s}^{-1}$)	Max. bottom shear stress (N m^{-2})
Irene	Cape Sable	10/15/99 5 PM	23	2.3	5.2
Frances	Cat Island	9/5/04 2 AM	31	4.7	8.5
Jeanne	Hutchinson Island	9/26/04 1 AM	33	2.5	8.5
Wilma	Cape Romano	10/24/05 11 AM	41	1.5	8.7

Severe storms can intensify the scouring effect on the sediment bed, degrade water quality, destroy SAV, and devastate the ecosystem balance. In addition, droughts can impact the lake's hydrodynamic patterns and water depths. Four major hurricanes in the past decade, Irene (1999), Frances and Jeanne (2004), and Wilma (2005), made landfall in southern Florida and impacted the Lake Okeechobee ecosystem (Table 1) [2,8]. These hurricanes, along with long-term droughts in 2000–2001 and 2007–2008, resulted in unexpected environmental and ecological consequences and led to major changes in sediment distribution, migration, and deposition, water quality variations, and structural changes in the submerged aquatic vegetation (SAV) and plankton communities [9]. The coupling effect of hurricanes and droughts on sediment bed and ecosystem stability may deeply affect the lake's sustainability [8].

This study presents a holistic assessment of the coupling effect of hurricanes and droughts on SAV variations and associated ecosystem changes in Lake Okeechobee, Florida, from 2001 to 2008. To promote region wide sustainable development, this analysis focused on: (1) how the coupled hurricane and drought impact changed the spatial and temporal distributions of SAV and (2) how the ecosystems responded to changing SAV patterns under coupled hurricane and drought impact. An expanded numerical model, the Lake Okeechobee Environment Model (LOEM), was developed and applied to link the spatial and temporal distributions of SAV in relation to natural and anthropogenic stressors.

2 WATER QUALITY ANALYSIS

Hurricane Irene in 1999 did not significantly impact water quality in Lake Okeechobee, because it did not stir up the consolidated sediment bed. The long-term impacts were seen in a 2- to 3-fold increase in turbidity and total phosphate in the 6 months that followed (Fig. 1); however, they returned to normal the following summer (2000). The monthly averages of turbidity and total phosphate increased 2- to 3-fold again in winter 2001 because the data were collected immediately following a cold front, which lasted about 6 months.

Hurricanes Frances (2004), Jeanne (2004), and Wilma (2005) had a long-term impact on the water quality and ecosystem balance in Lake Okeechobee. While hurricanes Frances and Jeanne loosened the sediment layers from the top down to 10–12 cm, Hurricane Wilma continuously cracked down on the consolidated sediment layers from 10–12 cm down to 25 cm at L9, which is a monitoring station located at the north-central area of the lake [2,8]. The top layer of the unconsolidated sediment mud turned into available sources of suspended solids, and these fine-grained materials became more susceptible to suspension or resuspension to the water column, even under mild wind conditions, providing a plentiful source of P to the water column. Due to the collective impact of hurricanes Frances, Jeanne, and Wilma, the turbidity and total phosphate has remained at high levels continuously for 3–4 years (Fig. 1). The available suspended sediment takes a long time to settle and

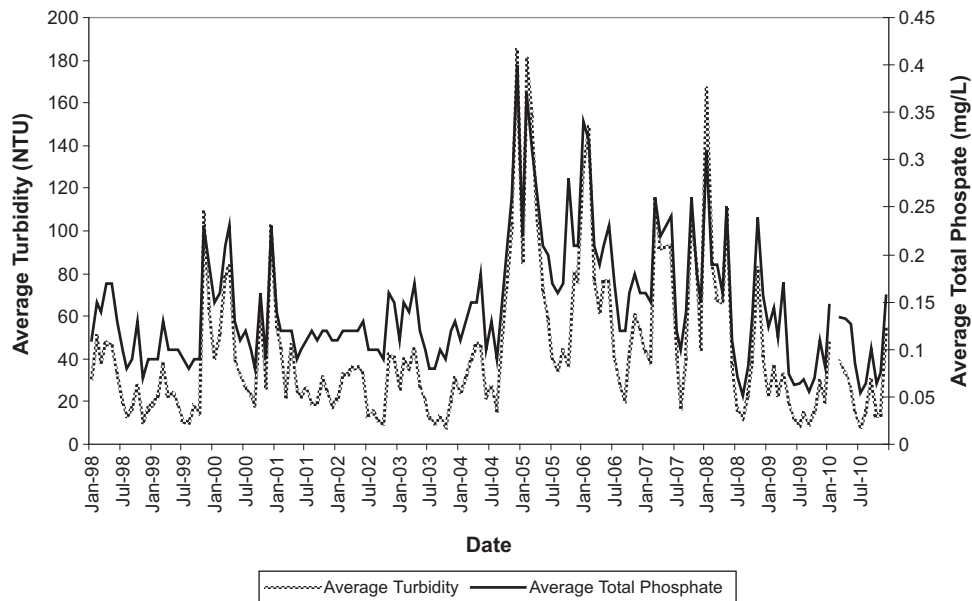


Figure 1: Covariations of monthly averages of turbidity and total phosphate in mud zone 1998 to 2010 [2].

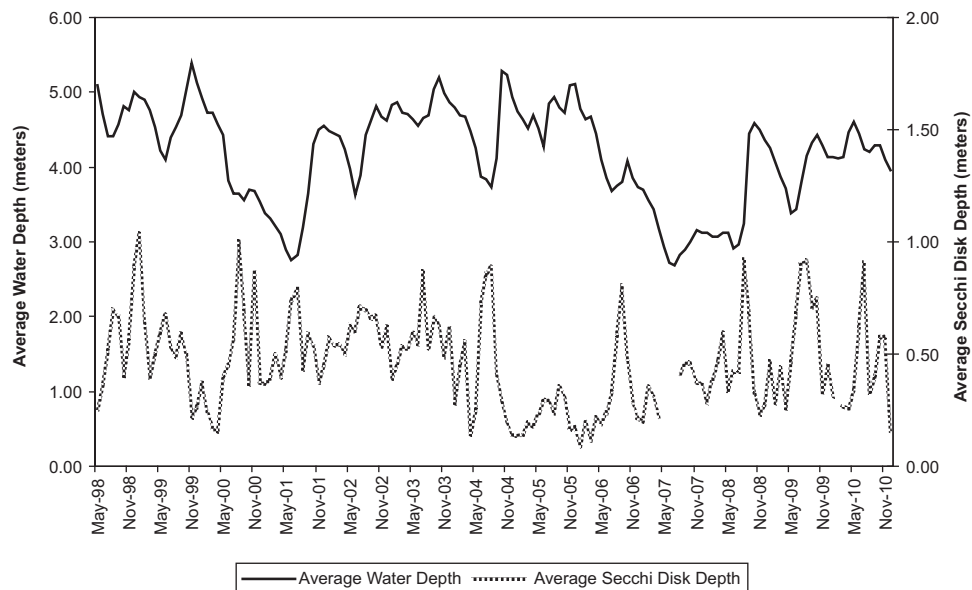


Figure 2: Monthly average Secchi disk depth and water depth in the transition zone from 1998 to 2010 [2].

consolidate, greatly reducing light transrance (Fig. 2), which further damages the habit of aquatic vegetation by lengthening the stress period and recovery time following a hurricane landfall. This event-based process has yet to end, even after 3–4 years.

3 ECOLOGICAL IMPACT ASSESSMENT

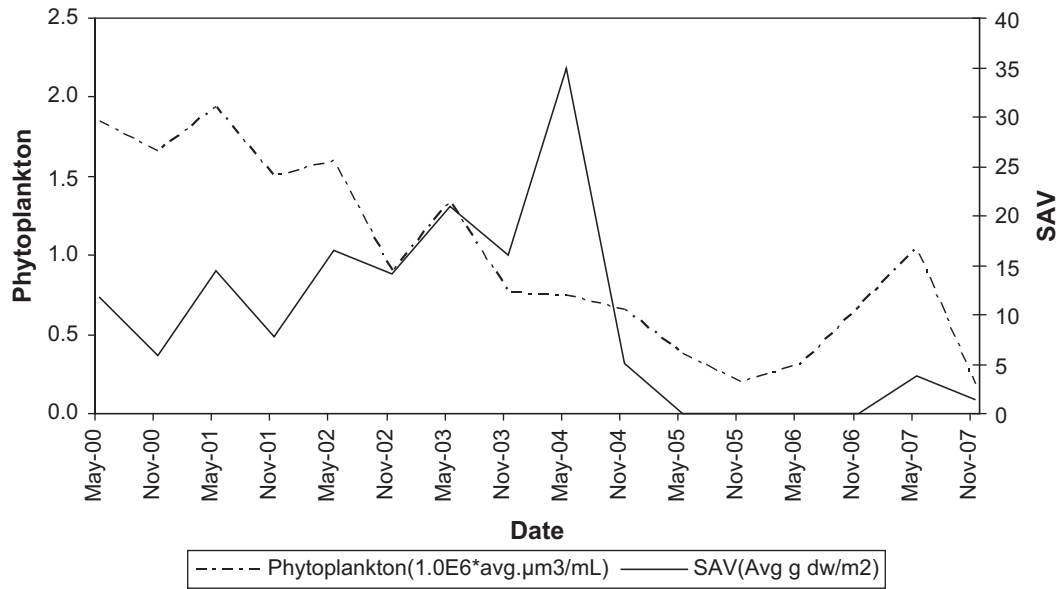
3.1 Structure change of Lake Okeechobee ecosystem

The drought impact in 2002 was deemed mild and did not significantly impact the SAV biomass (Fig. 3). The hurricanes' long-term impacts on water quality and SAV are significant, however, even several years after landfall. The three dominant species that mainly comprise the SAV biomass, *Chara* (a branch of macro algae), *Vallisneria* (eel grass), and *Hydrilla*, did not show any reduction in the following years after Hurricane Irene (Fig. 3); yet, the SAV biomass showed a sharp reduction in the years following hurricanes Frances and Jeanne in 2004 and Wilma in 2005 and never partially recovered until 2007 (Fig. 3). The series of hurricanes in 2004 and 2005 considerably increased the total suspended solids (TSS), decreased the Secchi disk depth (Fig. 2), and reduced the light transparency ratio in the littoral and near-shore regions, blocking SAV and phytoplankton growth. The average SAV biomass dropped from the pre-hurricane levels of 20 and 10 g dry m⁻² for summer and winter averages, respectively, to 4 g dry m⁻² by the end of winter 2004. The biomass further dropped to 0.1 g dry m⁻² after Hurricane Wilma and continued to decline to a level <0.02 g dry m⁻² through 2005 and 2006, due to the presence of high TSS that blocked the light penetration in the Lake. This low light situation lasted until summer 2007 when the drought impact dwindled gradually. The SAV in the near-shore regions (transition zone) located between the littoral zone and the mud zone were almost totally destroyed during the 2004–2005 hurricane season (Fig. 3).

The 3-year hurricane impact of high TSS and turbidity and low Secchi disk depth significantly from 2004 to 2007 stressed the lake's ecosystem and damaged the food chain of the lake to some extent. Populations of macrozooplankton and microzooplankton were also heavily impacted by the 2004 hurricanes Frances and Jeanne (Fig. 3). The population of macrozooplankton was reduced by 50%, while the microzooplankton population dropped nearly 70%. Both populations rebounded in summer 2005; however, they were destroyed again by Hurricane Wilma in October 2005. When the SVA biomass dropped to 4 g dry m⁻² in winter 2004–2005 and continued to decline to <0.02 dry m⁻² in winter 2005–2006, the population of phytoplankton in the lake also decreased sharply to 40 10E4 μ³ mL⁻¹ after the 2004 and 2005 hurricane seasons and continued to decline to 20 10E4 μ³ mL⁻¹ in winter 2005–2006. Nevertheless, the drought event in 2007 and 2008 triggered a fast recovery of the phytoplankton population, similar to that of SAV recovery because both SAV's and phytoplankton's driving factors are light attenuation, nutrient, and water depth. In general, the phytoplankton population grows faster than SAV so that the recovery rate should be more significant than SAV's, although the microzooplankton might suppress the growth rate of phytoplankton (Fig. 3). The population of macrozooplankton and microzooplankton recovered faster than SAV and phytoplankton, partially due to the reduced number of small fish, which are the natural predators of macrozooplankton and microzooplankton in the lake. In any circumstance, the Lake Okeechobee ecosystem has become more vulnerable to severe climate since the harsh damage from the 2004 and 2005 hurricane seasons followed by the drought impact.

The historical drought that occurred in 2007–2008 did not dramatically change the TSS, turbidity, and total phosphate, and the averages of these three water quality indicators were maintained at a level twice the normal range. However, the average water depth dropped significantly during the historical 2007–2008 drought event (Fig. 2), driving the lake stage so low that light could almost reach the lake bed, which allowed the SAV seeds to germinate and grow in the shallow water despite the high TSS and turbidity. The in-lake habitat conditions that had been disrupted by the hurricanes in 2004 and 2005 were gradually improved and recovered by the 2007–2008 drought events.

(a) Ecodynamics between SAV and phytoplankton.



(b) Ecodynamics between SAV and zooplankton.

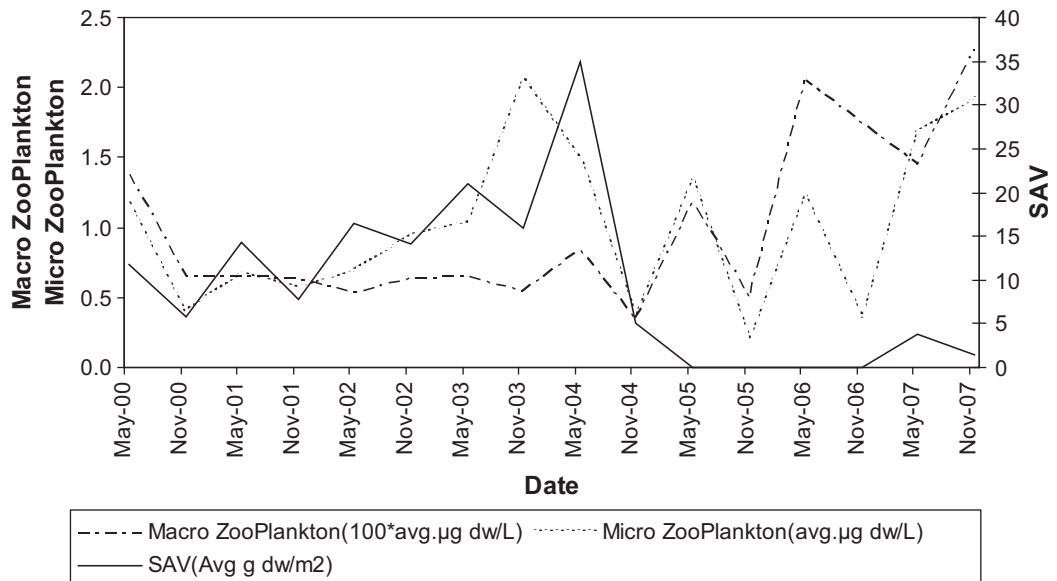


Figure 3: Interactions among SAV biomass, zooplankton, and phytoplankton in the water column from 2000 to 2007.

4 EXPANSION OF LOEM

4.1 Core module of LOEM

The LOEM is modified from the Environmental Fluid Dynamics Code (EFDC), a public-domain modeling package for simulating three-dimensional flow, transport, and biogeochemical processes in surface water systems [10]. This model solves the three-dimensional, vertically hydrostatic, free surface, turbulent averaged equations of motions for a variable density fluid. Dynamically coupled transport equations for turbulent kinetic energy, turbulent length scale, and temperature also are solved.

The two turbulence transport equations implement the Mellor-Yamada level 2.5 turbulence closure scheme [11,12]. The model is a variable-density, unsteady-flow model that uses the Boussinesq approximation, a hydrostatic pressure distribution, and the eddy-viscosity concept. Under the horizontal Cartesian coordinates and the vertical sigma coordinate, the governing continuity, momentum, and transport equations are used in the model [13-15]. The horizontal Cartesian coordinate form of governing equations used in the model for describing the continuity, momentum, and transport [15] are

$$\frac{\partial H}{\partial t} + \frac{\partial Hu}{\partial x} + \frac{\partial Hv}{\partial y} + \frac{\partial \omega}{\partial \sigma} = Q_H, \quad (1)$$

$$\frac{\partial(Hu)}{\partial t} + \frac{\partial(Huu)}{\partial x} + \frac{\partial(Huv)}{\partial y} + \frac{\partial(u\omega)}{\partial \sigma} - fHv = -H \frac{\partial(p + p_{atm} + \phi)}{\partial x} + \left(\frac{\partial z_b}{\partial x} + \sigma \frac{\partial H}{\partial x}\right) \frac{\partial p}{\partial \sigma} + \frac{\partial}{\partial \sigma} \left(\frac{A_v}{H} \frac{\partial u}{\partial \sigma}\right) + Q_x, \quad (2)$$

$$\frac{\partial(Hv)}{\partial t} + \frac{\partial(Huv)}{\partial x} + \frac{\partial(Hvv)}{\partial y} + \frac{\partial(v\omega)}{\partial \sigma} + fHu = -H \frac{\partial(p + p_{atm} + \phi)}{\partial y} + \left(\frac{\partial z_b}{\partial y} + \sigma \frac{\partial H}{\partial y}\right) \frac{\partial p}{\partial \sigma} + \frac{\partial}{\partial \sigma} \left(\frac{A_v}{H} \frac{\partial v}{\partial \sigma}\right) + Q_y, \quad (3)$$

$$\frac{\partial p}{\partial \sigma} = gH \frac{(\rho_w \rho_\sigma)}{\rho_0} = gHb, \text{ and} \quad (4)$$

$$(\tau_{xz}, \tau_{yz}) = \frac{A_v}{H} \frac{\partial}{\partial \sigma} (u, v) \quad (5)$$

where u (m s^{-1}) and v (m s^{-1}) are the horizontal velocity components in the Cartesian horizontal coordinates x (m) and y (m), respectively; b is buoyancy (kg m^{-3}); ω (m s^{-1}) is the vertical velocity in the stretched vertical coordinate σ ; z_s (m) and z_b (m) are the physical vertical coordinates of the free surface and bottom bed, respectively; g (m s^{-2}) is gravitational acceleration; H (m) is the total water column depth; and ϕ is the free surface potential ($\text{m}^2 \text{s}^{-2}$), which is equal to gz_s . The effective Coriolis acceleration f (s^{-1}) incorporates the curvature acceleration terms according to eqns (2) and (3); Q_H (m s^{-1}) represents volume sources and sinks, including rainfall, evaporation, infiltration, and lateral inflows and outflows having negligible momentum fluxes; Q_x ($\text{m}^2 \text{s}^{-2}$) and Q_y ($\text{m}^2 \text{s}^{-2}$) in eqns (2) and (3) represent optional horizontal momentum diffusion terms; p_{atm} (N m^{-2}) is the kinematic atmospheric pressure referenced to water density, while the excess hydrostatic

pressure in the water column is given by eqn (4); A_v ($\text{m}^2 \text{s}^{-1}$) is the vertical turbulent momentum diffusion coefficient that relates the shear stresses to the vertical shear of the horizontal velocity components in eqn (5); and ρ (kg m^{-3}) and ρ_o (kg m^{-3}) are actual and reference water densities, respectively.

Vertical boundary conditions, including bottom and wind stresses for the solution of the momentum equations, are based on the specification of kinematic shear stresses [15]. Wind speeds used in the wind stress calculation are the components of wind velocity at 10 m above the water surface [16]. The three-dimensional heat balance equation and formulations of heat fluxes are the same as those used in the calibration period [17]. The model uses heat flux formulations based on the National Oceanic and Atmospheric Administration Geophysical Fluid Dynamic Laboratory's atmospheric heat exchange formulation [18].

The transport equation in Cartesian coordinates for a suspended sediment class is

$$\begin{aligned} & \partial_t(HS) + \partial_x(HuS) + \partial_y(HvS) + \partial_z(wS) - \partial_z(w_sS) \\ & = \partial_x(HK_H\partial_xS) + \partial_y(HK_H\partial_yS) + \partial_z\left(\frac{K_v}{H}\partial_zS\right) + Q_s, \end{aligned} \quad (6)$$

where H is the water depth; u and v are the horizontal velocity components in the Cartesian horizontal coordinates x and y ; w_s is settling velocity; w is the vertical velocity in the stretched vertical coordinate; S (mg L^{-1}) is the suspended sediment concentration; K_v ($\text{m}^2 \text{s}^{-1}$) and K_H ($\text{m}^2 \text{s}^{-1}$) are the vertical and horizontal turbulent diffusion coefficients; and Q_s ($\text{mg L}^{-1} \text{m s}^{-1}$) represents external sources and sinks. Vertical boundary conditions for the sediment transport equation are

$$\begin{aligned} & -\frac{K_v}{H}\partial_zS - w_sS = J_o : z \approx 0 \\ & -\frac{K_v}{H}\partial_zS - w_sS = 0 : z = 1, \end{aligned} \quad (7)$$

where J_o ($=J_d + J_r$) ($\text{mg L}^{-1} \text{m s}^{-1}$) is the net sediment flux from the bed to the water column, which is equal to the summation of sediment deposition flux (J_d) ($\text{mg L}^{-1} \text{m s}^{-1}$) and sediment resuspension flux (J_r) ($\text{mg L}^{-1} \text{m s}^{-1}$). At the water surface, $z = 1$, the net zero flux condition means that there is no net transport across the free surface and, therefore, diffusion flux always counterbalances the settling flux. At the sediment bed, $z = 0$, the net sediment flux is equal to the summation of sediment erosion flux and sediment deposition flux. The sediment concentration profile is quite sensitive to erosion and deposition, which are the source or sink to the total mass in the sediment transport process. The net sediment flux formulation of noncohesive sediment [19] was applied to this study.

4.2 Modeling the SAV distribution

The SAV model incorporates three state variables: shoots (above the bed sediment), roots (in the bed sediment), and epiphytes (attached to the shoots). Shoots and epiphytes exchange nutrients with the water column component of the water quality model. Roots exchange nutrients with the bed sediment diagenesis component of the water quality model [20]. The kinetic mass balance equations for rooted plant shoots, roots, and epiphyte algae growing on the shoots are [21]

$$\frac{\partial(RPS)}{\partial t} = \left((1 - F_{PRPR}) \cdot P_{RPS} - R_{RPS} - L_{RPS} \right) RPS + JRP_{RS} \quad (8)$$

$$\frac{\partial(RPR)}{\partial t} = F_{PRPR} \cdot P_{RPS} \cdot RPS - (R_{RPR} + L_{RPR})RPR - JRP_{RS}, \text{ and} \quad (9)$$

$$\frac{\partial(RPE)}{\partial t} = (P_{RPE} - R_{RPE} - L_{RPE})RPE, \quad (10)$$

where t stands for time (day); RPS is the rooted plant shoot biomass (g C m^{-2}); F_{PRPR} is the fraction of production directly transferred to roots ($0 < F_{PRPR} < 1$); P_{RPS} is the production rate for plant shoots (day^{-1}); R_{RPS} is respiration rate for plant shoots (day^{-1}); L_{RPS} is the nonrespiration loss rate for plant shoots (day^{-1}); JRP_{RS} is the carbon transport positive from roots to shoots ($\text{g C m}^{-2} \text{ day}^{-1}$); RPR is rooted plant root biomass (g C m^{-2}); R_{RPR} is the respiration rate for plant roots (day^{-1}); L_{RPR} is the nonrespiration loss rate for plant roots (day^{-1}); RPE is the rooted plant epiphyte biomass (g C m^{-2}); P_{RPE} is the production rate for epiphytes (day^{-1}); R_{RPE} is the respiration rate for epiphytes (day^{-1}); and L_{RPE} is the nonrespiration loss rate for epiphytes (day^{-1}).

The governing equation for shoots, eqn (8), establishes a balance between sources and sinks of SAV biomass in the water column. The governing equation for roots, eqn (9), establishes a balance between sources and sinks of SAV biomass in the sediment bed. An additional state variable is used to account for shoot detritus at the bottom of the water column:

$$\frac{\partial(RPD)}{\partial t} = F_{RPSD} \cdot L_{RPS} \cdot RPS - L_{RPD} \cdot RPD, \quad (11)$$

where RPD is the rooted plant shoot detritus biomass (g C m^{-2}); F_{RPSD} is the fraction of shoot loss to detritus ($0 < F_{RPSD} < 1$); and L_{RPD} is the decay rate of detritus (day^{-1}).

A complete understanding of ecosystem processes and effects will require a careful integration of the results of water quality and SAV analysis, controlled bioassay experiments, and outputs from a spatially intensive Lake Okeechobee hydrodynamic, water quality, and SAV model. The LOEM [13,22,23], a spatial scale three-dimensional environmental model of the lake that provides the above crucial hydrodynamic information, was calibrated and verified by the South Florida Water Management District to predict long-term hydrological and nutrient conditions, SAV, and environmental impacts in Lake Okeechobee under different management scenarios of physical, chemical, and biological (submerged vegetation) conditions [24–26]. Besides, three components are required to simulate SAV growth: an SAV model that describes SAV biomass growth and decay; a water quality model that provides light, water temperature, nutrients, and other forcing functions for the SAV model; and a coupling algorithm that links the water quality model to the SAV model. All three components were calibrated and verified as described in Jin et al. [26] and Ji [27].

The model could be used to examine the time sequence of concentrations of stressors as they are mixed throughout the lake, and thereby identify the regions where biota are expected to be most affected under different management scenarios (high and low stages, hurricanes, and sediment dredging and management). Simulation runs were carried out from 1999 to 2008 using an expanded LOEM model.

5 ECODYNAMICS OF SAV ASSOCIATED WITH EVENT-BASED LOEM MODELING ANALYSIS

SAV is an important habitat, providing a refuge for juvenile fish and shellfish as well as a food source for fish and waterfowl. Consequently, the assessment of SAV provides a direct link between water quality (nutrients, chlorophyll a , and suspended sediments) and ecologically and economically important species. The extent of SAV in a water system varies directly with water clarity and

inversely with water depth. The amount of TSS, nutrients, and algae in the water column affect water clarity and play a major role in controlling SAV growth. As a consequence, the extent of SAV coverage is often an important performance measure for evaluating the success of nutrient reduction efforts and water quality management in an ecosystem.

The LOEM generated event-based spatial distributions of SAV, leading to the exploration of spatiotemporal changes of SAV associated with velocity fields under hurricane and drought impacts in Lake Okeechobee. With the aid of the expanded LOEM model, a series of events can collectively delineate the ecodynamics of SAV evolutionary pathway (Figs 4,5,6,7,8,9,10,11). The graph begins with the

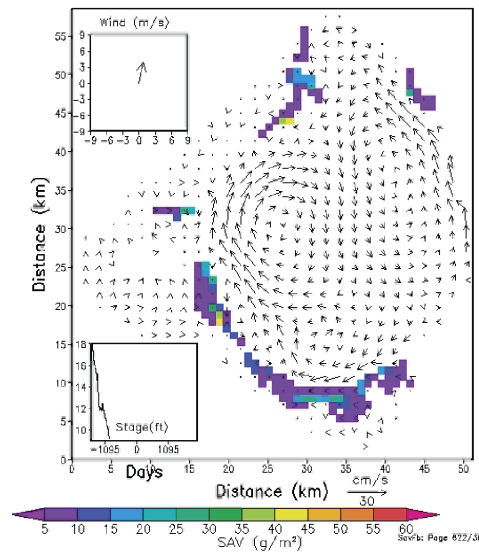


Figure 4: Low Lake stage 5/4/2001, SAV area = 27,156 Acres.

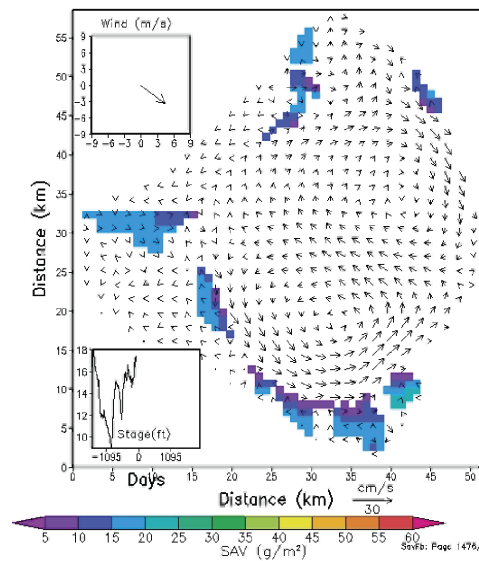


Figure 5: High Lake stage 10/14/2003, SAV area = 40,156 Acres.

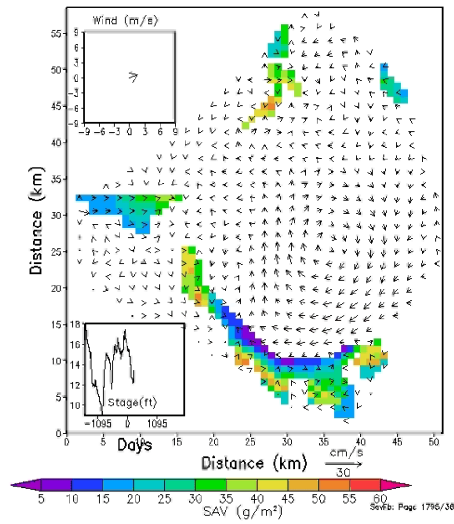


Figure 6: Before Frances, 8/30/2004, SAV area = 51,267 Acres.

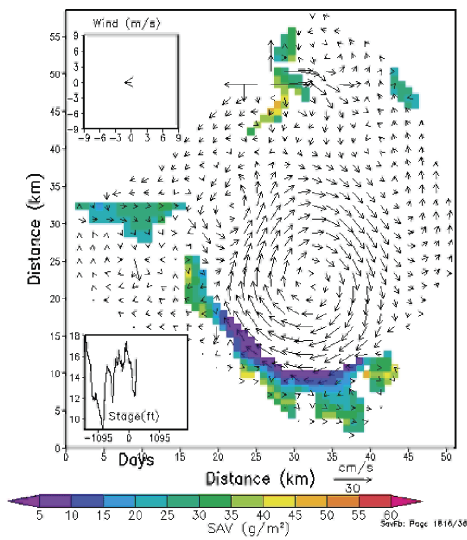


Figure 7: After Frances, 9/20/2004 SAV area = 50,888 Acres.

2001 drought's impact giving rise to a low water level in May 2001 (i.e. event 1 described in Fig. 4), which limited the area of SAV coverage to 27,156 acres. The subsequent recovery of water level promoted the growth of SAV in October 2003 (i.e. event 2 described in Fig. 5), raising the area of SAV coverage to 40,156 acres. Before the landfall of Hurricane Frances in August 2004 (i.e. event 3 described in Fig. 6), the area of SAV was enlarged to 51,267 acres, with denser SAV in the littoral zone. After the landfall of Hurricane Frances, larger velocity field were observed, which destroyed part of the SAV in the littoral zone and reduced the total area of SAV to 50,888 acres (i.e. event 4 described

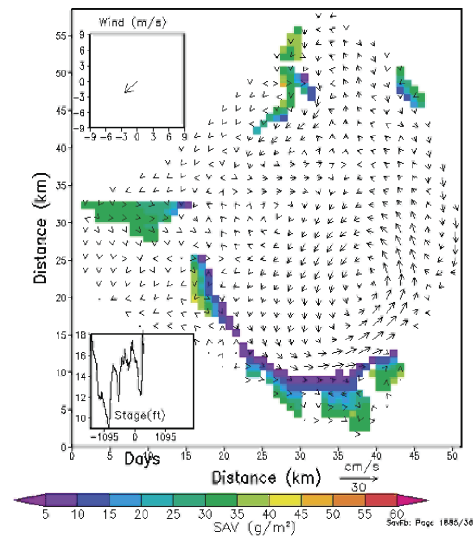


Figure 8: After Frances, 11/27/2004, SAV area = 45,645 Acres.

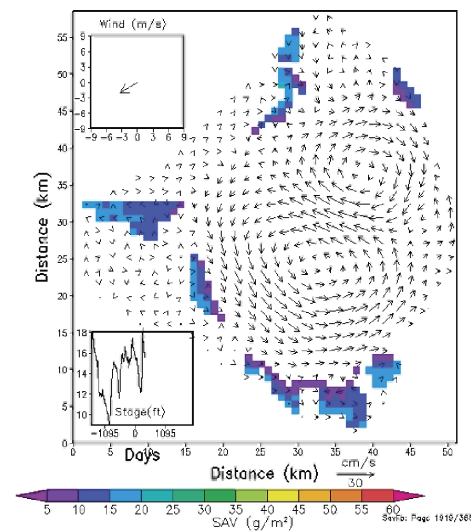


Figure 9: After Frances, 1/1/2005, SAV area = 40,065 Acres.

in Fig. 7). Although the SAV reduction was not dramatic immediately after landfall, the negative impact persisted over a period of time. At the end of 2004, the residual effect of Hurricane Frances further decreased the area of SAV to 45,645 acres (i.e. event 5 described in Fig. 8). After 2 months, the area of SAV shrank closer to 40,000 acres (i.e. event 6 described in Fig. 9). Immediately before Wilma in early November 2005, the area of SAV shrank further to 13,235 acres due to the extremely high turbidity and low-light penetration in the previous year (i.e. event 7 described in Fig. 10). However, after the landfall of Hurricane Wilma, the situation continued to worsen, and only 9,246 acre of SAV

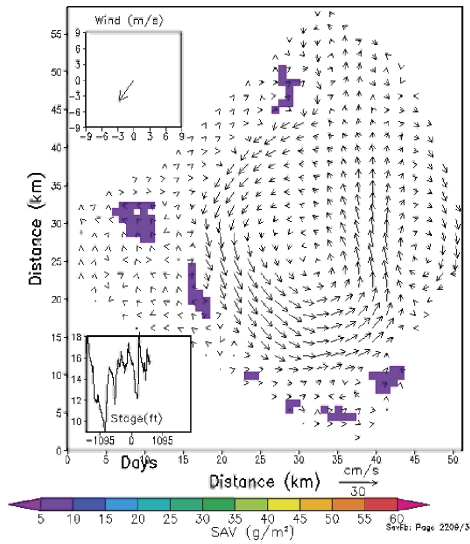


Figure 10: Right before Wilma, 10/15/2005, SAV area = 13,235 Acres.

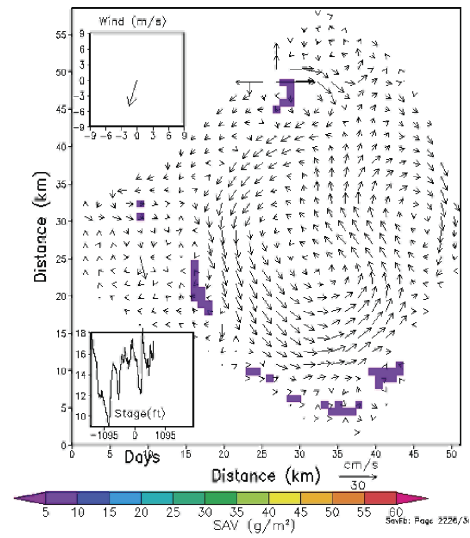


Figure 11: After Wilma, 10/26/2005, SAV area = 9,246 Acres.

remained (i.e. event 8 described in Fig. 11). The turbidity and total phosphate remained continuously at high levels for 3–4 years due to the collective impact of hurricanes Frances, Jeanne, and Wilma, which significantly depressed the recovery of SAV to the levels observed in the early 2000s.

6 CONCLUSIONS

SAV is often a desirable component of shallow lakes and wetlands, and therefore management activities are often directed to ensure their continual presence. Hurricane Irene in 1999 did not have a

significant impact on the SAV in Lake Okeechobee, because the consolidated sediment bed was not affected; neither did the drought in 2000–2001 influence the water quality in Lake Okeechobee. The long-term impacts caused by hurricane Irene extended only to the TSS, turbidity, and total phosphate increasing 2- to 2.5-fold in the 6 months following landfall; however, the SAV biomass did not show any reduction in the following years. In contrast, the series of hurricanes from 2004 to 2005 resuspended a tremendous amount of nonconsolidated sediment, resulting in a dramatic increase in TSS, turbidity, and total phosphate within the water column of the lake. Hurricane Wilma generated the largest storm surge and bottom shear stresses in the past decade, which significantly impacted water quality in the lake, although its persistence time (1.5 day) was shorter than hurricanes Frances (4.7 days) and Jeanne (2.5 days). Hurricanes also brought a large amount of rainfall, run-off, and debris from the drainage basin. The wind–wave effect of hurricanes stirred up the consolidated sediment layer in the mud zone of the lake, and turned the consolidated sediment into nonconsolidated sediment, fine grained particles that are hard to settle and easy to resuspend even under mild wind conditions. The mechanism of sediment and high lake level led to high TSS and turbidity sufficient to reduce light transparency and depress the coverage of SAV. The above factors contributed to the decline of biomass of SAV, small fish, and phytoplankton from the post-hurricane period until late 2008, the end of the long-term drought.

The 2004–2005 hurricanes destroyed the SAV community and the near-shore plants. The SAV biomass was reduced to nearly zero for two continuous years until 2008. The SAV growth area also showed significant decline in 2005–2006. During this period most fish lost nesting areas or breeding grounds, and juvenile fish could not find an SAV shelter area to escape predators and survive. The SAV that survived in the transition zone gradually recovered during summer 2007 due to the historical drought of the lake, during which TSS, turbidity, and total phosphate remained relatively stable at nearly double the normal range. Although during 2007–2008 the SAV area recovered to a normal range, the SAV intensity (biomass) was still very low.

Overall, the LOEM model for the estimation of SAV areas and biomass performed quite well in this study. The in-lake habitat conditions and ecosystem restoration, which had been disrupted by hurricanes, may be improved by means of water level control and SAV recovery. With this advance Vai modeling analysis, it is possible to achieve SAV growth in the lake through managing the lake stage within a more ideal range based on the knowledge derived by the modeling outputs. This pathway can be simulated using the expanded LOEM model, contributing to possible biomanipulation too in the future.

REFERENCES

- [1] Schottler, S. & Engstrom, D., A chronological assessment of Lake Okeechobee (Florida) sediments using multiple dating markers. *Journal of Paleolimnol*, **36**, pp. 19–36, 2006. doi: <http://dx.doi.org/10.1007/s10933-006-0007-5>
- [2] Chang, N.B., Makkeasorn, A. & Shah, T., Lake Okeechobee sediment profile characterization. Technical Report for Contract 4100000079, submitted to South Florida Water Management District, West Palm Beach, Florida, 2008.
- [3] Aumen, N.G., The history of human impacts, lake management, and limnological research on Lake Okeechobee, Florida (USA). *Archival of Hydrobiology, Advances in Limnology*, **45**, pp. 1–16, 1995.
- [4] Havens, K.E., Aumen, N.G., James, R.T. & Smith, V.H., Rapid ecological changes in a large subtropical lake undergoing cultural eutrophication. *AMBIO*, **25**, pp. 150–155, 1996.
- [5] Maceina, M.J. & Soballe, D.M., Wind-related limnological variation in Lake Okeechobee. *Lake and Reservoir Management*, **6**, pp. 93–100, 1990. doi: <http://dx.doi.org/10.1080/07438149009354699>

- [6] Steinman, A.D., Havens, K.E., Aumen, N.G., James, R.T., Jin, K-R., Zhang, J. & Rosen, B.H., Phosphorus in Lake Okeechobee: sources, sinks, and strategies. *Phosphorus Biogeochemistry in Subtropical Ecosystems*, eds K.R. Reddy, G.A. O'Conner, and C.L. Schelske, Albany, GA: Lewis Publishers, 1999.
- [7] Jin, K.R. & Wang, K.H., Wind generated waves in Lake Okeechobee. *Journal of AWRA*, **34(6)**, pp. 1–12, 1998.
- [8] Jin, K.R., Chang, N.B., Ji, J., & Thomas, J.R., Hurricanes affect sediment and environments in Lake Okeechobee. *Critical Reviews in Environmental Science and Technology*, **41(S1)**, pp. 382–394, 2011. doi: <http://dx.doi.org/10.1080/10643389.2010.531222>
- [9] James, R.T., Chimney, M.J., Sharfstein, B., Engstrom, D.R., Schottler, S.P., East, T., & Jin, K.R., Hurricane effects on a shallow lake ecosystem, Lake Okeechobee, Florida (USA). *Fundamental and Applied Limnology, Archiv fur Hydrobiologie*, **172/4**, pp. 73–287, 2008.
- [10] Hamrick, J.M., Estuarine environmental impact assessment using a three-dimensional circulation and transport model. *Estuarine and Coastal Modeling, Proceedings of the 2nd International Conference*, eds M.L. Spaulding et al., American Society of Civil Engineers, New York, pp. 292–303, 1992.
- [11] Mellor, G.L. & Yamada, T., Development of a turbulence closure model for geophysical fluid problems. *Reviews of Geophysics and Space Physics*, **20**, pp. 851–875, 1982. doi: <http://dx.doi.org/10.1029/RG020i004p00851>
- [12] Galperin, B., Kantha, L.H., Hassid, S. & Rosati, A., A quasi-equilibrium turbulent energy model for geophysical flows. *Journal of Atmospheric Sciences*, **45**, pp. 55–62, 1988. doi: [http://dx.doi.org/10.1175/1520-0469\(1988\)045<0055:AQETEM>2.0.CO;2](http://dx.doi.org/10.1175/1520-0469(1988)045<0055:AQETEM>2.0.CO;2)
- [13] Jin, K.R. & Ji, Z.G., Case Study: modeling of sediment transport and wind-wave impact in lake okeechobee. *Journal of Hydraulic Engineering, ASCE*, **130(11)**, pp. 1055–1067, 2004. doi: [http://dx.doi.org/10.1061/\(ASCE\)0733-9429\(2004\)130:11\(1055\)](http://dx.doi.org/10.1061/(ASCE)0733-9429(2004)130:11(1055))
- [14] Jin, K.R., Ji, Z.G. & Hamrick, J.H., Modeling winter circulation in Lake Okeechobee, Florida. *Journal of Waterway, Port, Coastal, and Ocean Engineering, ASCE*, **128(3)**, pp. 114–125, 2002. doi: [http://dx.doi.org/10.1061/\(ASCE\)0733-950X\(2002\)128:3\(114\)](http://dx.doi.org/10.1061/(ASCE)0733-950X(2002)128:3(114))
- [15] Hamrick, J.M., & Wu, T.S., Computational design and optimization of the EFDC/HEM3D surface water hydrodynamic and eutrophication models. *Next Generation Environmental Model and Computational Methods*. eds G. Delich, and M.F. Wheeler, Philadelphia, PA: society of industrial and applied mathematics, pp. 143–161, 1997.
- [16] Dean, R.G. & Dalrymple, R.A., *Water Wave Mechanics for Engineers and Scientists*, World Scientific Publishing Co., Singapore, 1991.
- [17] Jin, K.R., Hamrick, J.H. & Tisdale, T.S., Application of three-dimensional hydrodynamic model for Lake Okeechobee, *Journal of Hydraulic Engineering, ASCE*, **126(10)**, pp. 758–77, 2000. doi: [http://dx.doi.org/10.1061/\(ASCE\)0733-9429\(2000\)126:10\(758\)](http://dx.doi.org/10.1061/(ASCE)0733-9429(2000)126:10(758))
- [18] Rosati, A.K., & Miyakoda, K., A general circulation model for upper ocean simulation. *Journal of Physical Oceanography*, **18**, pp. 1601–1626, 1988. doi: [http://dx.doi.org/10.1175/1520-0485\(1988\)018<1601:AGCMFU>2.0.CO;2](http://dx.doi.org/10.1175/1520-0485(1988)018<1601:AGCMFU>2.0.CO;2)
- [19] Mehta, A.J., Hayter, E.J., Parker, W.R., Krone, R.B., & Teeter, A.M., Cohesive sediment transport. I: Process Description. *Journal of Hydraulic Engineering*, **115**, pp. 1076–1093, 1989. doi: [http://dx.doi.org/10.1061/\(ASCE\)0733-9429\(1989\)115:8\(1076\)](http://dx.doi.org/10.1061/(ASCE)0733-9429(1989)115:8(1076))
- [20] Cerco, C.F., Johnson, B.H. & Wang, H.V., Tributary refinements to the Chesapeake Bay Model. Technical Report, U.S. Army Corps of Engineers Waterway Experiment Station, Vicksburg, MS., ERDC TR-02-4, 2002.
- [21] Hamrick, J.M. & Mills, W.B., A Rooted Aquatic Plant and Epiphyte Algae Sub-Model for EFDC, unpublished technical notes, 2001.

- [22] Jin, K.R. & Ji, J., Calibration and verification of a spectral wind-wave model for Lake Okeechobee. *Journal of Ocean Engineering*, **28(5)**, pp. 573–586, 2001. doi: [http://dx.doi.org/10.1016/S0029-8018\(00\)00009-3](http://dx.doi.org/10.1016/S0029-8018(00)00009-3)
- [23] Jin, K.R., Ji, Z.G. & Hamrick, J.H., Modeling winter circulation in Lake Okeechobee, Florida. *Journal of Waterway, Port, Coastal, and Ocean Engineering*, ASCE, **128(3)**, pp. 114–125, 2002. doi: [http://dx.doi.org/10.1061/\(ASCE\)0733-950X\(2002\)128:3\(114\)](http://dx.doi.org/10.1061/(ASCE)0733-950X(2002)128:3(114))
- [24] Jin, K.R. & Ji, Z.G., Case study: modeling of sediment transport and wind-wave impact in Lake Okeechobee. *Journal of Hydraulic Engineering*, ASCE, **130(11)**, pp. 1055–1067, 2004. doi: [http://dx.doi.org/10.1061/\(ASCE\)0733-9429\(2004\)130:11\(1055\)](http://dx.doi.org/10.1061/(ASCE)0733-9429(2004)130:11(1055))
- [25] Jin, K.R. & Ji, Z.G., Application and validation of a 3-D model in a shallow lake. *Journal of Waterway, Port, Coastal, and Ocean Engineering*, ASCE, **131(5)**, pp. 213–225, 2005. doi: [http://dx.doi.org/10.1061/\(ASCE\)0733-950X\(2005\)131:5\(213\)](http://dx.doi.org/10.1061/(ASCE)0733-950X(2005)131:5(213))
- [26] Jin, K.R., Ji, Z.G. & James, T.R., Three dimensional water quality modeling of a large shallow lake. *Journal of Great Lakes Research*, **33(1)**, pp. 28–45, 2007. doi: [http://dx.doi.org/10.3394/0380-1330\(2007\)33\[28:TWQASM\]2.0.CO;2](http://dx.doi.org/10.3394/0380-1330(2007)33[28:TWQASM]2.0.CO;2)
- [27] Ji, Z.-G., *Hydrodynamics and Water Quality: Modeling Rivers, Lakes, and Estuaries*. Hoboken, New Jersey: John Wiley & Sons, Inc., p. 676, 2008.